An Investigation into the Role of Dielectric Resonance in Parallel Imaging

F. Wiesinger[1], P-F. Van de Moortele[2], G. Adriany[2], N. De Zanche[1], C. Snyder[2], T. Vaughan[2], K. Ugurbil[2], K. P. Pruessmann[1]

[1]Institute for Biomedical Engineering, ETH and University Zurich, Zurich, Switzerland, [2]Center for MR Research (CMRR), University of Minnesota, Minneapolis, Minnesota, United States

INTRODUCTION:

Ultra-high field strengths and parallel imaging are expected to form a considerable synergy. This has recently been emphasized both by theoretical investigations (1-3) and practical experiments (4,5). However, a key concern raised by these studies is whether or not dielectric resonance interferes with the efficient use of parallel imaging at ultra-high field strength. In the presence of a significant dielectric resonance, coil sensitivity profiles have significant contributions from resonant eigenmodes of the object. These are specific for the geometry of the object rather than for the positioning and geometry of the coil (6). Accordingly, coil sensitivities become more similar, hence potentially preventing the efficient use of parallel imaging. In order to study these effects, parallel SENSE imaging (7) has been performed in the presence of dielectric resonance in two different phantom geometries on a 7 Tesla MRI system. In particular, the impact of conductivity-related dielectric resonance damping was investigated by graded addition of sodium chloride.

METHODS:

Two phantoms of different symmetry were chosen: a 3 liter glass flask of spherical symmetry and a 1 gallon (3.785 liters), approximately cuboid plastic container of mirror-symmetry. The dielectric resonance spectra of the water-filled phantoms were measured using a small search coil connected to a calibrated HP 4396A network analyzer as suggested in Ref. (8). By replacing small amounts of distilled water (ε_r=79 at 300MHz) by ethanol (ε_r=24 at 300MHz), the frequency of a nearby resonant mode was adjusted to the 7 Tesla Larmor frequency. The effect of conductivity on resonance damping was investigated by introducing small amounts of sodium chloride to achieve saline concentrations of 20mM and 50mM; a 50mM saline water solution corresponds approximately to average in-vivo brain conductivity at 300MHz (9). All imaging experiments were performed on a 7 Tesla magnet (Magnex Scientific, UK), equipped with a Varian Inova console (Palo Alto, CA) and Siemens gradient amplifiers (Erlangen, Germany). Data acquisition was performed with an eight-element, straight-line, microstrip TEM transceive coil array (4,10). Tuning and matching could be performed robustly in all situations. Images were acquired using a gradient-recalled echo (GRE) sequence (TR=50ms, TE=5ms, 3mm slice thickness, matrix=256x256). Coil sensitivity maps were determined following a procedure described in Ref. (5). Parallel imaging performance was quantified by calculating the local geometry factor for reduction factors (R) in the range between 1 and 5 with noise correlation taken into account (7).

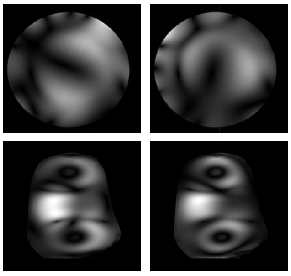

***Fig.1**: Dielectric resonance patterns (0mM NaCl).*

RESULTS:

Figure 1 shows the dielectric resonance patterns in the two phantom geometries, as revealed by single-coil image data in the case of 0mM salinity: For the spherical flask (top row) data from two different coil elements are shown in a central transverse slice. A two-lobe mode can be clearly appreciated. Small additional modulations near the surface are due to destructive interference during RF excitation, reflecting non-ideal transmit phase adjustments. For the cuboid container (bottom row), a coronal slice is shown, likewise from two different coil elements. Again, a clear higher-order dielectric resonance can be appreciated. However, unlike the spherical phantom the resonance pattern does not change significantly with coil position. Figure 2 compares calculated mean geometry factors between the spherical (left) and the cuboid phantom (right) in a central transverse slice. Three different saline concentrations are shown: 0mM (black solid line), 20mM (red dashed line) and 50mM (green dotted line). For the spherically symmetric phantom, the calculated geometry factors are all in the same range. However, for the mirror-symmetric container the geometry factor improves significantly from 0mM to 20mM and remains approximately constant for higher salinity

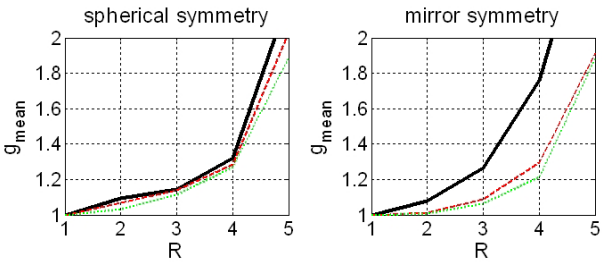

***Fig.2**: Parallel imaging performance comparison.*

DISCUSSION:

The discrepancy in parallel imaging performance between the two phantom geometries (Fig.2) can be related to characteristics of the specific dielectric resonance patterns (Fig.1). For the spherical symmetric flask, the excited dielectric mode appears to be spherically degenerate, with the consequence that the resonance pattern in the coil sensitivities still depends on the coil position. In particular, in the two images shown in Fig.1, top row, it can be recognized that the corresponding coil elements are arranged perpendicularly to each other. Accordingly, in this degenerate eigenmode, the individual coil sensitivities are similarly orthogonal for 0mM, 20mM and 50mM salinity, resulting in almost identical, favorable geometry factors (Fig.2 left). Conversely, in the mirror-symmetric container a non-degenerate eigenmode was excited. In the case of 0mM salinity, the single-coil images differ only by small sensitivity variations, while the underlying mode structure is the same for all coil elements (Fig.1 bottom row). Correspondingly, the coil sensitivity profiles are less orthogonal, resulting in still moderate but enhanced geometry factors for the lossless case. However, inducing conductivity by adding 20mM sodium chloride significantly improves the geometry factor. Further increasing the saline concentration to 50mM leaves the geometry factor nearly unchanged (Fig.2 right). The human head exhibits only approximate mirror symmetry. Therefore, non-degenerate resonance modes are expected for brain imaging, indicating the less favorable g factor behavior. However, according to the right plot in Fig.2, the intrinsic tissue conductivity may be expected to sufficiently damp dielectric resonance modes in the head to a sub-critical level for parallel imaging.

CONCLUSION:

(I) The impact of dielectric resonance on parallel imaging performance appears to depend on the degeneracy of the resonant mode. A high level of mode degeneracy was observed to be favorable for parallel imaging. In the more general, non-degenerate case, dielectric resonance resulted in still moderate but enhanced geometry factors in a lossless object. (II) Independent of the dielectric mode degeneracy, minor amounts of sodium chloride stabilize the geometry factor at usual levels. This suggests that under in-vivo conditions dielectric resonance may not be a major specific problem for parallel imaging, in accordance with Refs. (4,5). This result is also in agreement with conclusions drawn in Ref. (9). There it was observed that the RF field distribution in the human head at ultra-high fields is predominantly characterized by damped traveling wave interference and near-field contributions rather than by resonant standing wave patterns.

REFERENCES: [1] Wiesinger, F., et al, Proc ISMRM 10 (2002): p.191, [2] Ohliger, M.A. et al, Proc ISMRM 10 (2002): p.2387, [3] Ledden, P., et al, Proc ISMRM 10 (2002): p.324, [4] Adriany, G., et al, Proc ISMRM 11 (2003): p.474. [5] Wiesinger, F., et al, Proc ESMRMB 20 (2003): p.39, [6] Richtmyer, R.D., J Appl Phys 10: 391-398 (1939), [7] Pruessmann, K.P., et al, MRM 42:952-962 (1999), [8] Hoult D.I., et al, Concepts Magn Reson 12: 173-187 (2000), [9] Yang, Q.X., et al, MRM 47: 982-989 (2002), [10] Vaughan, J.T., 'RF Coil for Imaging System', US Patent Serial No. 6,633,161 (2003).

ACKNOWLEDGEMENT: This work was supported by EUREKA/KTI E!2061/4178.1 INCA-MRI, SEP Life Science TH7/02-2, NIH grant P41 RR08079, R01 HL33600, R01 EB00331, R33 CA94318, R01 EB00473, R01 CA94200, W.M Keck Foundation and the MIND Institute.